J Solid State Electrochem (2014) 18:1049–1056
DOI 10.1007/s10008-013-2354-2

ORIGINAL PAPER

Electrodeposition of cobalt oxide nanoparticles on reduced graphene oxide: a two-dimensional hybrid for enzyme-free glucose sensing

Su-Juan Li · Ji-Min Du · Jing Chen · Nan-Nan Mao · Meng-Jie Zhang · Huan Pang

Received: 9 October 2013 / Revised: 1 November 2013 / Accepted: 2 December 2013 / Published online: 13 December 2013

Abstract Based on the extraordinarily properties of graphene, cobalt oxide nanoparticles (CoO_xNPs)/graphene-modified electrode was prepared by electrodeposition of CoO_xNPs on the glassy carbon surface previously modified with electrochemically reduced graphene oxide (ERGO), which was characterized by scanning electron microscopy (SEM), cyclic voltammetry (CV), and electrochemical impedance spectroscopy. It was found that a large amount of CoO_xNPs with diameter less than 100 nm was uniformly grown on the surface of graphene nanosheets. The as-prepared CoO_xNPs/ERGO hybrids were applied to construct an enzyme-free sensor for glucose detection in alkaline solution. The developed glucose sensor shows a short response time (less than 5 s), a high sensitivity of 79.3 μA mM^{-1} cm^{-2}, a detection limit of 2 μM (S/N = 3), and good selectivity to prevent from the interference of some species including ascorbic acid, uric acid, dopamine, and sodium chloride. Importantly, favorable reproducibility and long-term performance stability were also obtained. Application of the proposed sensor in monitoring urine glucose was also demonstrated.

Keywords Electrodeposition · Cobalt oxide · Graphene · Enzyme-free · Glucose

Electronic supplementary material The online version of this article (doi:10.1007/s10008-013-2354-2) contains supplementary material, which is available to authorized users.

S.-J. Li (✉) · J.-M. Du · J. Chen · N.-N. Mao · M.-J. Zhang · H. Pang
Key Laboratory for Clearer Energy and Functional Materials of Henan Province, College of Chemistry and Chemical Engineering, Anyang Normal University, Anyang 455000, Henan, China
e-mail: lisujuan1981@gmail.com

Introduction

In the past decades, driven by the rising demands for advanced blood sugar detector for clinical diagnosis and personal care and the urgent requirements for monitoring and control of food preparation processes, the development of efficient glucose sensors with high sensitivity, fast response, and excellent selectivity has gained special focus for analytical scientist [1, 2]. Although few optical [3, 4] strategies have been developed, electrochemical methods are still considered to be the most convenient and effective tool for measuring the glucose levels because of its high sensitivity, rapid response, good reliability and selectivity, simple instrumentation, and low cost [5, 6]. Electrochemical glucose sensors can be mainly classified into two categories: glucose oxidase (GOD)-based sensing and enzyme-free glucose sensing. In spite of the low detection limit, the GOD biosensors often suffer from stability and reproducibility issues that originated from the intrinsic nature of the enzymes [7]. Nowadays, enormous interest has been paid on the development of enzyme-free glucose sensors, which would exhibit conveniences and advantage to avoid the enzyme electrode drawbacks based on direct electrocatalytic oxidation of glucose at electrode surface.

Recent advancement in the fabrication of nanomaterials has provided new platforms for enzyme-free glucose sensing applications. Currently, various noble metals (Au, Pt, Ag, Pd) [8–11], transition metal and its oxides (Ni, Cu, CuO, NiO, Co_3O_4) [12–16], and alloys (Pt–Pd, Pt–Au, Au–Ag) [17–19] have been explored as electrode materials to construct a variety of enzyme-free glucose sensors. Among these, a major concern in practical nonenzymatic glucose sensing is focused on constructing high-performance devices using inexpensive and resourceful transition metal oxides catalysts. Recently, cobalt oxides (CoO_x), with intriguing electronic, optical, electrochemical, and electrocatalytic properties, has attracted

considerable attention because of their excellent electrocatalytic performance toward glucose. Nanostructured CoO_x with high specific surface area and enhanced electrochemical activity is particularly attractive for exerting its electrocatalytic properties. For example, Ding et al. [16] fabricated electrospun Co_3O_4 nanofibers for sensitive and selective glucose detection. Hou et al. [20] synthesized Co_3O_4 nanoparticles by using MOFs as template and utilized it for direct glucose and H_2O_2 detection. Dong et al. [21] synthesized a three-dimensional (3D) graphene/Co_3O_4 nanowire composite using a simple hydrothermal procedure, which serves as a free-standing monolithic electrode for high-performance supercapacitor and enzymeless glucose detection. Lee et al. [22] prepared CoOOH nanosheet array on a cobalt substrate via a simple alkaline treatment and demonstrated its potential in non-enzymatic glucose sensing. Therefore, the development of novel CoO_x nanostructure-based material for accurately detecting glucose is still urgent.

Graphene, a two-dimensional monolayer of sp^2-hybridized carbon atoms, has attracted enthusiastic interest since its discovery in 2004 [23]. In particular, graphene-based hybrid nanomaterials are of scientific and industrial interest because of their enhanced properties arising from the large specific surface area, high electrical and thermal conductivities. With appropriate design, the hybrid nanomaterials can exhibit improved performance due to the synergistic contribution of two or more functional components [24, 25]. To date, great efforts have been made to incorporate graphene into composite materials and explore their applications in various fields including metal nanoparticles [26–28], metal oxides [29, 30], conducting polymers [24, 31], carbon nanotubes [32], and quantum dots [33].

Inspired by the remarkable properties of graphene, we reason that when combined with CoO_xNPs, graphene-based heterostructure may present enhanced performance for application in amperometric enzyme-free glucose biosensors. Various CoO_x-reduced graphene oxide (GO) nanocomposites have been successfully constructed in previous reports [34–36]. Herein, highly distributed CoO_xNPs were electrochemically synthesized on the surface of electrochemically reduced graphene oxide (ERGO)-modified glassy carbon electrode and applied in the enzyme-free glucose sensor. The well-distributed CoO_xNPs can be easily and fully accessing to glucose, and amplifying the electrochemical signal for glucose determination. In addition, an efficient electrical network through CoO_xNPs directly anchoring on the surface of graphene can promote the electron transfer rate and accordingly improve the detection sensitivity. Therefore, a highly sensitive and selective glucose sensor based on CoO_xNPs/ERGO hybrids was obtained in alkaline solution. The facile and green preparation method, highly sensitive, fast, stable, and reproducible of the present CoO_xNPs/ERGO-based sensor promise to potential applications in the development of sensors for enzyme-free detection of glucose.

Experimental

Reagents and apparatus

Graphite powder (spectral requirement, Shanghai Chemicals) was used for synthesizing GO and ERGO. Glucose, ascorbic acid (AA), dopamine (DA), and uric acid (UA) were purchased from Sigma Aldrich. NaOH and Cobalt (II) chloride anhydrous were purchased from Sinopharm Chemical Reagent (Shanghai, China). All of these reagents were of analytical grade and used as received. Unless otherwise stated, ultrapure water (18.2 MΩ cm) produced by a Milli-Q system was used as the solvent throughout this work.

Scanning electron microscopy (SEM) was conducted by JSM-6701 F (Japan) for surface morphology observations. Electrochemical experiments were performed on a CHI 660D electrochemical station (Shanghai Chenhua, China) with a conventional three-electrode system. The CoO_xNPs/ERGO hybrid-modified glassy carbon electrode (CoO_xNPs/ERGO/GCE) was used as the working electrode. A Pt wire and a saturated calomel electrode (SCE) acted as the counter and reference electrodes, respectively.

Synthesis of CoO_xNPs/ERGO hybrid-modified electrode

The GO was synthesized from natural graphite powder based on a modified Hummers method as presented by Kovtyukhova and colleagues [37]. As-synthesized GO was dispersed in water, giving a yellow brown dispersion with a concentration of 1 mg ml^{-1} by an ultrasonic technique. A 10 μl portion of the resulting GO dispersion was dropped onto a pretreated bare GCE and dried at room temperature to obtain the GO-modified GCE (GO/GCE). Here, prior to the surface modification, GCE was polished with 0.3 and 0.05 μm alumina slurries, respectively, and then ultrasonically cleaned in water. The ERGO-modified electrode (ERGO/GCE) was prepared by scanning the potential of the GO/GCE between -1.5 and 0 V versus SCE at a scan rate of 100 mV s^{-1} for 20 cycles in 0.1 M KCl solution. After that, repetitive potential cycling (30 cycles at 100 mV s^{-1} at potential range between 1.1 and -1.1 V) in 0.1 M pH 7 phosphate-buffered saline solution containing 1 mM cobalt chloride was used for electrodeposition CoO_x nanoparticles on the surface of ERGO (CoO_xNPs/ERGO) according to the previous work [38, 39]. The cyclic voltammograms (CVs) of corresponding deposition curves have been presented in the supporting materials for Fig S1. The increasing redox peaks with potential cycles indicate the successful deposition of CoO_xNPs on ERGO surfaces. After deposition, the CoO_xNPs/ERGO hybrid-modified electrode was rinsed with distilled water. For comparison, a bare GCE was employed under the same deposition conditions to obtain CoO_xNP-modified electrode (CoO_xNP/GCE).

Electrochemistry measurements

Cyclic voltammetry and amperometric experiments were carried out at room temperature. A certain volume of stock solution of glucose and 10 ml supporting electrolyte were added into an electrochemical cell, and then the three-electrode system was inserted into the cell. The cyclic voltammetry was carried out to investigate the electrochemical response of the hybrid-modified electrode toward glucose. The amperometric experiment was performed to achieve the quantitative analysis.

Results and discussion

Characterization of the CoO_xNPs/ERGO hybrid-modified electrode

Fig. 1 shows the typical SEM images of electrodeposited CoO_xNPs on ERGO-modified glassy carbon electrode with different magnification. The image recorded at lower magnification (Fig 1a) indicates that the wrinkled graphene sheets have been homogeneously decorated with CoO_xNP by the present electrodeposition method. The higher-magnification SEM image (Fig 1b) reveals that the size of the nanoparticles is less than 100 nm, and several large agglomerated particles are also observed on the image in addition to well-distributed small particles. As we can see, the size of large agglomerated particles varies from under 100 nm to slightly less than 500 nm. The formation of CoO_xNPs on the ERGO-modified electrode was further checked by recording CV of the modified electrode in alkaline solution without cobalt ions. The obtained voltammogram is almost the same as others reported in the literature [16, 39]. As shown in Fig. 2a, three oxidation peaks appeared at about 0.10, 0.40, and 0.67 V during the anodic potential scan. These peaks correspond to the conversion between four different cobalt oxidation phases of $Co(OH)_2$, Co_3O_4, CoOOH, and CoO_2, which are stable at alkaline solution. During the reverse cathodic scan, two reduction peaks at 0.60 and 0.30 V were observed, which are attributed to the reduction of the various CoO_x species formed during the anodic scan. As reported, the redox reactions of II/V at 0.4/0.3 V and III/IV at 0.67/0.6 V can be formulated as $Co_3O_4 + OH^- + H_2O \rightarrow 3CoOOH + e^-$ and $CoOOH + OH^- \rightarrow CoO_2 + H_2O + e^-$. The irreversible oxidation peak at 0.1 V is due to the reaction $3Co(OH)_2 + 2OH^- \rightarrow Co_3O_4 + 4H_2O + 2e^-$. With an increase of the scan rate, both of the oxidation and reduction currents of peak II/V increase linearly (data shown in Fig 2b), suggesting a surface-controlled electron transfer process.

Electrochemical impedance spectroscopy (EIS) can exhibit the impedance changes during the modification processes, which is further used for the investigation of the electrode interface. The interface can be modeled by an equivalent circuit (shown in the inset of Fig. 3). This equivalent circuit includes the ohmic resistance of the electrolyte (R_s), the electron transfer resistance (R_{et}), the double layer capacitance (C_{dl}), and Warburg impedance (Z_w). The EIS includes a semicircular part and a linear part. The semicircular part at higher frequency corresponds to the electron-transfer limited process, and the diameter is equivalent to the R_{et}. The linear part at lower frequency corresponds to the diffusion process. Here, the R_{et} was concerned because the electron transfer properties of the modified materials is the most wanted to be known. As shown in Fig. 3, the R_{et} value was got as 145 Ω on the bare GCE. While on the CoO_xNPs/GCE, the R_{et} values were increased to 200 Ω, which was due to the presence of semiconducting CoO_x that lowered the electron transfer rate of $Fe(CN)_6^{3-/4-}$. For ERGO/GCE, the highly conductive graphene sheets significantly decreased the R_{et} values to only 103 Ω. However, the CoO_xNPs/ERGO hybrid-modified electrode showed a very low R_{et} of 99 Ω, lower than the values of both the single component of ERGO and CoO_xNPs. The results confirmed that an efficient electrical network through CoO_xNPs direct anchoring on the surface of graphene facilitates the electron-transfer.

Electrocatalytic oxidation of glucose on the CoO_xNPs/ERGO hybrid-modified electrode

The electrocatalytic activity of the CoO_xNPs/ERGO hybrid-modified electrode toward the oxidation of glucose in an

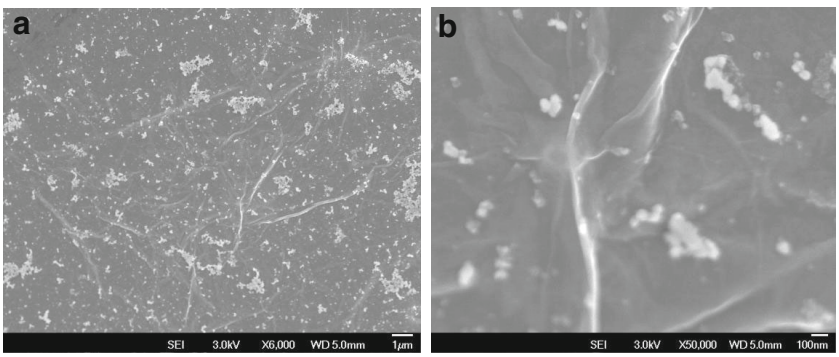

Fig. 1 SEM images of the electrodeposited cobalt oxide nanoparticles on ERGO-modified (CoO_xNPs/ERGO) glassy carbon electrode with low (**a**) and high (**b**) magnification

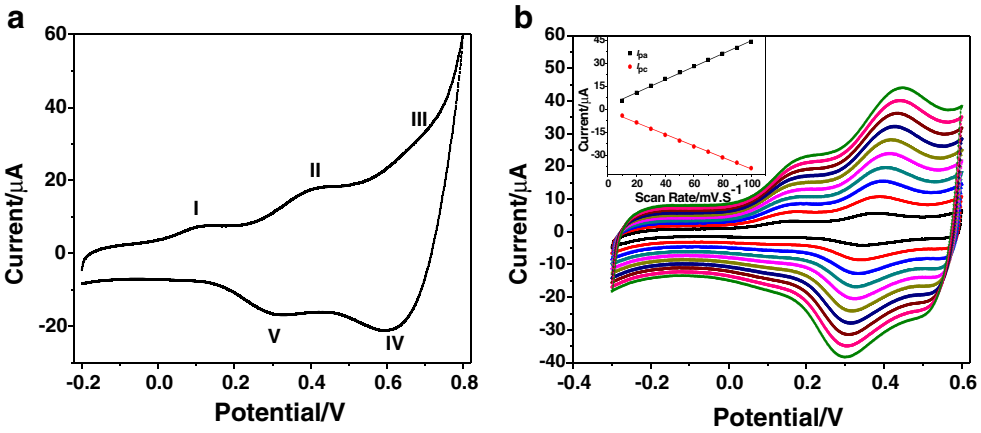

Fig. 2 **a** CV of CoO_xNPs/ERGO hybrid-modified electrode in 0.05 M NaOH at a scan rate of 50 mV s^{-1}, **b**: CVs of CoO_xNPs/ERGO hybrid-modified electrode in 0.05 M NaOH at different scan rates from 10 to 100 mV s^{-1}, the inset shows the relationship of redox currents of peak II/V with scan rates

alkaline medium was investigated. For comparison, the ERGO/GCE and CoO_xNPs/GCE were also conducted. Fig. 4 shows the CV responses of the (a) ERGO/GCE, (b) CoO_xNPs/GCE, and (c) CoO_xNPs/ERGO/GCE in the absence (black curve) and presence (red curve) of 2.0 mM glucose at a scan rate of 50 mV s^{-1}. As can be observed, the response of ERGO/GCE toward glucose is very limited and the oxidation of glucose requires a very high positive potential, which will lead to a very slow electrode kinetic. In contrast, the CoO_xNPs/GCE and CoO_xNPs/ERGO/GCE exhibited obvious electro-oxidation of glucose with a notable enhancement of the oxidation current starting from 0.40 to 0.80 V upon the addition of 2 mM glucose. As elegantly explained by Ding et al. [16], this is due to glucose oxidation to gluconolactone catalyzed by conversion of CoO_2 to CoOOH (redox pair III/IV): $2CoO_2 + C_6H_{12}O_6$ (glucose) → $2CoOOH + C_6H_{10}O_6$ (gluconolactone). Comparing the CV response of glucose to the above three electrodes (Fig. S2), it is clear that the CoO_xNPs/ERGO/GCE showed the largest electrocatalytic response for glucose oxidation starting from

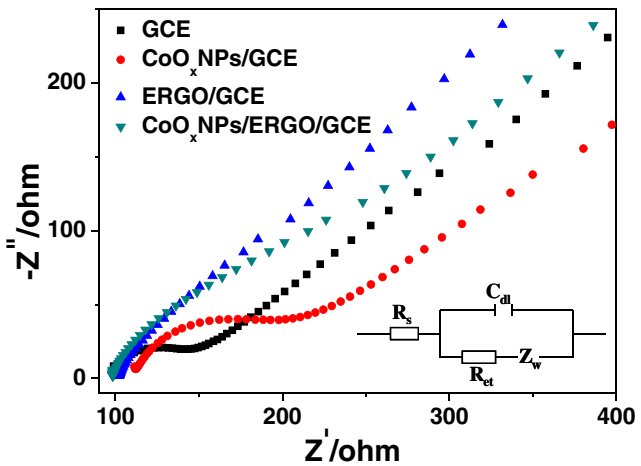

Fig. 3 The EIS of the bare GCE, CoO_xNPs/GCE, ERGO/GCE, and CoO_xNPs/ERGO/GCE in 5 mM $Fe(CN)_6^{3-/4-}$ and 0.1 mol/L KCl solution in the frequency range swept 10^5–0.1 Hz

0.40 to 0.80 V. In addition, the amperometric responses for successive additions of 50 μM glucose in 0.05 M NaOH at a constant potential of +0.60 V were obtained for ERGO/GCE, CoO_xNPs/GCE, and CoO_xNPs/ERGO/GCE. As displayed in Fig 4d, the largest current response for 50 μM glucose was obtained at CoO_xNPs/ERGO/GCE, which is consistent with the CV results. Such enhanced electrocatalytic performance of the CoO_xNPs/ERGO hybrids may be ascribed to a synergistic effect between graphene and the loaded CoO_x nanoparticles, which includes high catalytic active sites for the glucose oxidation provided by the well-distributed and high-loading amount of CoO_x nanoparticles and fast electron transfer channel offered by an efficient electrical network through CoO_xNPs directly anchoring on the surface of graphene. Here, the effect of ERGO in hybrid materials is forming an efficient electrical network for immobilization of highly distributed CoO_xNPs. The large surface area and high conductivity of ERGO makes the electron transfer rate of CoO_xNPs/ERGO/GCE obviously higher than that of CoO_xNPs/GCE, which facilitates the electrooxidation of glucose correspondingly.

The electrocatalytic behavior of CoO_xNPs/ERGO/GCE toward different concentrations of glucose was studied by CV. As shown in Fig. 5, the oxidation currents of glucose starting from 0.4 to 0.8 V increase gradually with increasing concentrations of glucose from 0 to 3 mM, which lays out prospect for the subsequent quantitative analysis. Prior to nonenzymatic glucose detection, experimental parameters possibly influencing the analytical performance of the fabricated nonenzymatic sensor were optimized. The effect of applied potentials was first systemically studied on the amperometric response of the CoO_xNPs/ERGO hybrid electrode to glucose. Constant potential chronoamperometry was performed at the potential range from +0.55 to +0.70 V with a settle interval of 0.05 V of the CoO_xNPs/ERGO hybrids electrode for successive additions of 50 μM glucose (Fig. 6a). Obviously, the current response of 50 μM glucose increases significantly from 0.55 to 0.60 V, and increases gradually from 0.60 to 0.65 V, then keeps nearly the

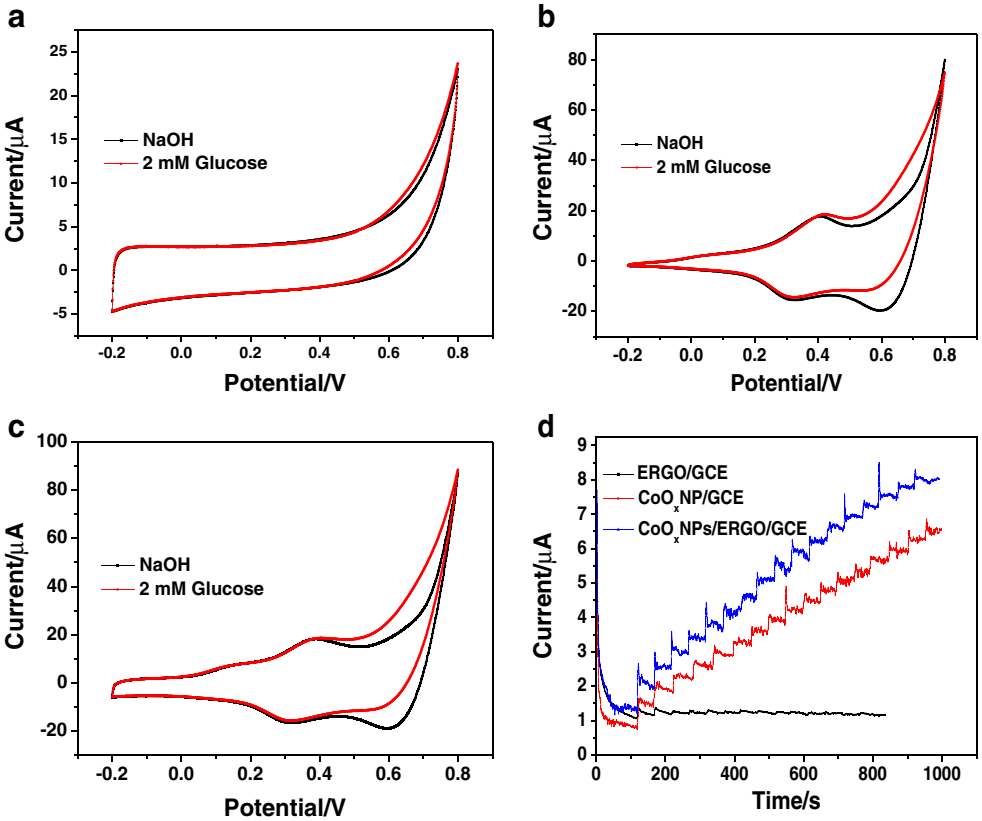

Fig. 4 CV responses of the ERGO/GCE (**a**), CoO_xNPs/GCE (**b**), and CoO_xNPs/ERGO/GCE (**c**) in the absence (*black curve*) and presence (*red curve*) of 2.0 mM glucose at a scan rate of 50 mV s^{-1}. **d** Amperometric responses of the above three electrodes to successive additions of 50 μM glucose in 0.05 M NaOH at +0.60 V. 0.05 M NaOH was used as the supporting electrolyte

equilibrium at 0.65 V. Considering that the maximum current response and that high applied potential may oxidize endogenous interfering species, +0.60 V was thus chosen as the optimum applied detection potential.

In nonenzymatic glucose sensors, an alkaline medium can be favorable for improving the electrocatalytic activity of the transition metal-based catalysts. Hence, the impact of NaOH concentrations was investigated in amperometric measurements for detecting 0.25 mM glucose. As shown in Fig. 6b, the amperometric currents increase correspondingly when the electrolyte concentration increases from 0.005 to 0.05 M because glucose is more easily oxidized and the electrocatalytic activity of CoO_x nanoparticles is greatly enhanced at high pH. The CV results also indicate negative shifts of the redox couple of CoO_x at higher pH (Fig. S3), meaning lower applied potential is needed for amperometric sensing. However, with further increasing the electrolyte concentration from 0.05 to 0.1 M, the amperometric current is reduced. The possible reason is that too much OH^- can block the further electroadsorption of glucose anion and result in a decrease in current response signal.

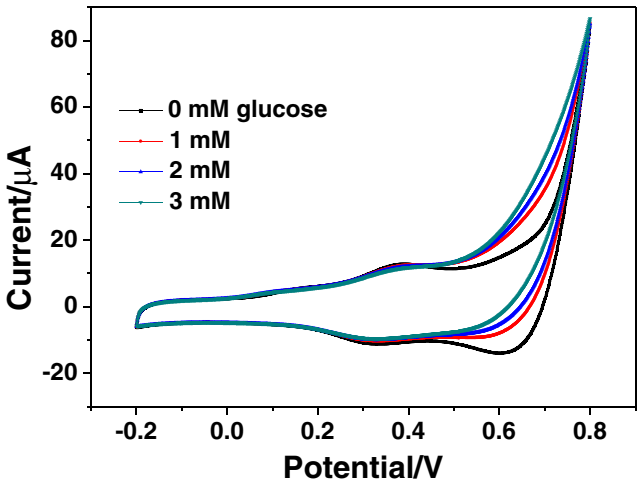

Fig. 5 CVs of CoO_xNPs/ERGO/GCE in the absence and presence of different concentrations of glucose

Amperometric sensing of glucose

Under the above optimized conditions, amperometric responses upon successive additions of glucose into constantly stirred NaOH solutions were recorded. Fig.7a shows the amperometric response of the CoO_xNPs/ERGO hybrids electrode (holding at 0.60 V) upon additions of glucose to increasing concentrations in 0.05 M NaOH. Well-defined amperometric currents increasing stepwise with the level of glucose are obtained. The CoO_xNPs/ERGO hybrids exhibit sensitive and rapid current response to glucose addition, achieving a steady-state current in less than 5 s, demonstrating efficient catalytic ability of the CoO_xNPs/ERGO hybrids electrode for

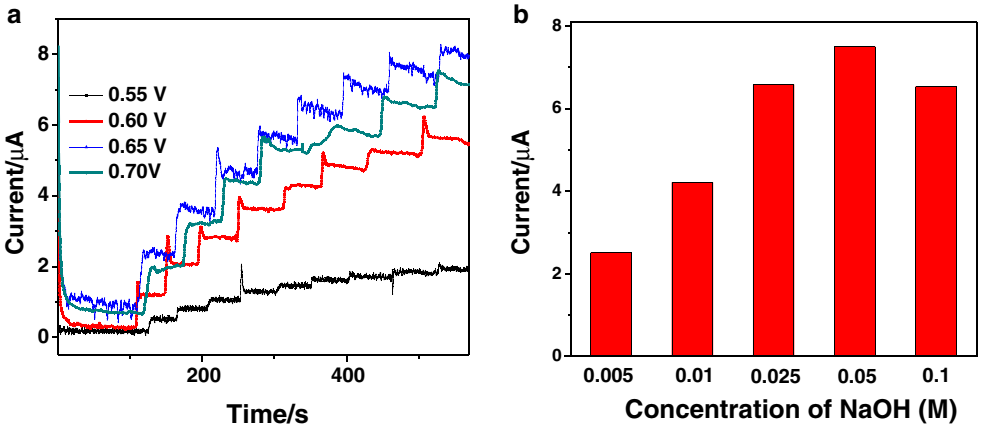

Fig. 6 **a** Amperometric responses of CoO_xNPs/ERGO/GCE upon the successive additions of 50 μM glucose at different applied potentials. **b** The current response of CoO_xNPs/ERGO/GCE toward 0.25 mM glucose at +0.60 V under different NaOH concentrations

glucose electro-oxidation. The inset of Fig 7a presents the relationship between the amperometric response of glucose and its concentration. It can be found that the current increases significantly with the increase of glucose when its total concentration is lower than 550 μM, and then increases gradually to a saturation with further increasing the glucose concentration, because the electrode surface partially covered by the adsorbed reaction intermediates cannot provide sufficient sites to accommodate the incoming glucose. The calibration curve for the electrochemical responses of the CoO_xNPs/ERGO hybrids electrode to glucose is shown in Fig 7b. The response to glucose exhibits a good linear range from 10 to 550 μM with a correlation coefficient of 0.9942 and a slope of 5.6 μA mM^{-1}. A sensitivity of 79.3 μA mM^{-1} cm^{-2} is obtained by dividing the slope of the linear regression equation by the electroactive surface area, which was higher than 1.06, 36.25, 8.59 μA mM^{-1} cm^{-2} for the enzymeless glucose electrochemical sensor based on FeOOH nanowires [40], Co_3O_4 nanofibers [16], and Cu-CuO nanowire composites [41]. The limit of detection (LOD) is estimated to be as low as 2 μM, based on the signal/noise value of 3 (S/N=3). For comparison, enzyme-free glucose sensing performances based on various nanomaterials from previous reports and our present study are shown in Table 1. As observed, the performance of the present CoO_xNPs/ERGO-based sensor is comparable to other similar CoO_x non-enzyme sensors (such as Refs. [16, 21, 22]) in view of sensitivities, linear range, and the LOD. For example, the present sensitivity is higher than that based on Co_3O_4 nanofibers [16]. In addition, the present linear range is obviously higher than that based on 3D graphene/CoO_x [21] and the LOD is significantly lower than that obtained on CoOOH nanosheets [22]. The high sensitivity and low LOD are believed to be attributed to the high catalytic activity of CoO_xNPs and the electrical network formed through CoO_xNPs directly distributing on the surface of graphene, which not only can keep their intrinsic excellent electrical conductivity but also facilitate CoO_xNPs easily accessing to glucose. Therefore, the electrochemical response for glucose oxidation can be greatly enhanced.

Interference test and detection of glucose in urine sample

Some interference often co-existing with glucose in a biological sample, such as DA, AA, and UA, could be easily oxidized and interfere with glucose detection. In the physiological sample, glucose concentration (4–7 mM) is generally much higher than those of interfering species. Therefore, the influence of 0.1 mM interference species on the current

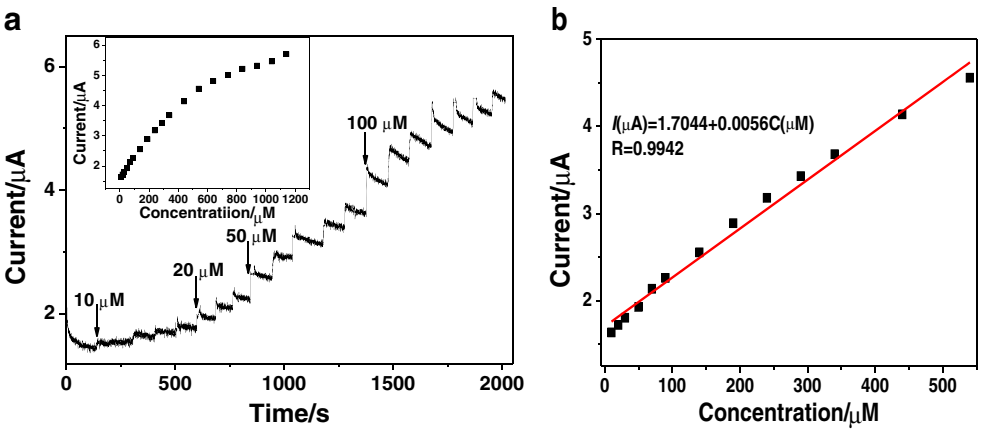

Fig. 7 **a** Amperometric response of the CoO_xNPs/ERGO hybrids electrode (holding at 0.60 V) upon addition of glucose to increasing concentrations in 0.05 M NaOH, the inset is the relationship between the amperometric response of glucose and its concentration. **b** The corresponding calibration curve

Table 1 Comparison of enzyme-free glucose sensing performances based on various nanomaterials

Electrode materials	Response time (s)	Potential (V)	Sensitivity (μA mM^{-1} cm^{-2})	Linear range (mM)	LOD (μM)	Reference
Co_3O_4 nanofibers	7	+0.59	36.25	0.001–2	0.97	[16]
3D graphene/CoO_x	–	+0.58	3390	0–0.08	0.025	[21]
CoOOH nanosheets	<4	+0.40	341	0.03–0.7	30.9	[22]
FeOOH nanowires	–	+0.4	12.13	0.015–33	15	[40]
Cu/CuO nanowire composite	<5	+0.3	8.59	0.1–12	50	[41]
Ti/TiO_2 nanotube array/Ni	–	+0.55	200	0.1–1.7	4	[42]
CuO nanorods	<10	+0.60	371.43	0.004–8	4	[43]
CoO acicular nanorods	20–40	+0.50	571.8	0.2–3.5	0.058	[44]
CoO_xNPs/ERGO	<5	+0.60	79.3	0.01–0.55	2	This work

response of 1 mM glucose was evaluated. Besides, chloride ions can poison most of the non-enzymatic glucose sensors based on precious metals and alloys, the influence of high concentration (0.1 M) of NaCl on the amperometric detection of glucose was also investigated. From the current response in Fig. 8, a remarkable glucose signal was obtained comparing to the other four interfering species. Compared to 1 mM glucose, the interfering species yielded current response ranging from 11.6 % (0.1 mM AA), 3.8 % (0.1 mM UA), 3.4 % (0.1 M NaCl) to 7.9 % (0.1 mM DA).

The inter-electrode reproducibility investigation was conducted by comparing the response currents of six CoO_xNPs/ERGO hybrids electrodes prepared under the same conditions. The relative standard deviation (RSD) of response for amperometric determination of 50 μM of glucose was 6.2 %. In addition, eight measurements of 50 μM glucose using the same electrode yielded a RSD of 4.5 %. These results indicated excellent intra-electrode and inter-electrode reproducibility. Furthermore, the long-term stability of developed electrode was studied by analyzing its amperometric response after 1-month storage. The results showed only 5.8 % decrease in the current response to 50 μM glucose. This good stability and repeatability make the modified electrode feasible for practical applications.

In order to investigate the possible application of this biosensor in clinical analysis, the CoO_xNPs/ERGO hybrid electrode has been employed to the detection of glucose spiked in human urine sample. The urine samples were obtained from a healthy woman. There was no glucose level detected in the blank urine samples. Therefore, 5 mM standard solution of glucose was spiked in the urine sample. The sample was examined in 0.05 M NaOH solution by amperometric measurement at a potential of 0.60 V. Generally, 100 μl of urine sample was added into 10 ml of 0.05 M NaOH solution, and then 20 μl of 10 mM standard glucose solution was successively added into the sample. The results were presented in Table 2. As can be seen, the recovery of the spiked glucose to the urine sample was in the range of (95.5–102.0)%, indicating the accuracy of the present method.

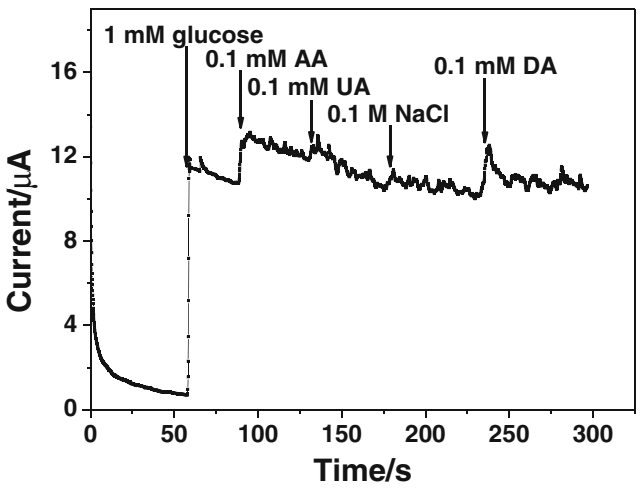

Fig. 8 Amperometric responses of the CoO_xNPs/ERGO hybrids electrode to successive additions of 1 mM glucose, 0.1 mM AA, 0.1 mM UA, 0.1 mM NaCl, 0.1 M DA, and 0.1 mM DA in 0.05 M NaOH at +0.60 V

Conclusions

In summary, a graphene-based heterostructure made of CoO_xNPs electrodeposited on ERGO surface have been successfully fabricated. The method for preparation of CoO_xNPs/ERGO is green, rapid, and controllable by adjusting the exterior electrochemical parameters. The prepared CoO_xNPs/ERGO hybrids electrode exhibits favorable electrocatalytic properties for glucose oxidation in alkaline media. The low

Table 2 Determination of glucose in a human urine sample (n=3)

Spiked (mM)	Detected (mM)	RSD (%)	Recovery (%)
5.00	4.92	3.94	98.4
7.00	6.95	3.62	101.5
9.00	8.86	4.29	95.5
11.0	10.9	4.07	102.0

detection limit, high detection sensitivity and reproducibility, and good selectivity of the as-prepared glucose sensor make the hybrids a good candidate for the construction of enzyme-free sensor for glucose detection. Since the relatively narrow linear range (up to 550 μM) for detecting glucose, efforts are underway in our laboratory to optimize the performance of CoO_xNPs-based sensors and especially to widen the linear detection range.

Acknowledgments We would like to acknowledge the financial support from the National Natural Science Foundation of China (No. 21105002, 21201010), the fund project for Henan Key Technologies R&D Programme (122102310516, 12B150002), and the Innovative Foundation for the College students of China and Anyang Normal University (201310479012, ASCX/2013-Z43).

References

1. Li Y, Song YY, Yang C, Xia XH (2007) Electrochem Commun 9: 981–988
2. Heller A, Feldman B (2008) Chem Rev 108:2482–2505
3. Evans ND, Rolinski OJ, Birch DJS (2005) Biosens Bioelectron 20: 2555–2565
4. Steiner MS, Duerkop A, Wolfbeis OS (2011) Chem Soc Rev 40: 4805–4839
5. Wang G, He X, Wang L, Gu A, Huang Y, Fang B, Geng B, Zhang X (2013) Microchim Acta 180:161–186
6. Nie H, Yao Z, Zhou X, Yang Z, Huang S (2011) Biosens Bioelectron 30:28–34
7. Siqueira JR, Caseli L, Crespilho FN, Zucolotto V, Oliveira ON (2010) Biosens Bioelectron 25:1254–1263
8. Liu A, Ren Q, Xu T, Yuan M, Tang W (2012) Sens Actuators B Chem 162:135–142
9. Park S, Chung TD, Kim HC (2003) Anal Chem 75:3046–3049
10. Quan H, Park SU, Park J (2010) Electrochim Acta 55:2232–2237
11. Gutés A, Carraro C, Maboudian R (2011) Electrochim Acta 56: 5855–5859
12. Niu X, Lan M, Zhao H, Chen C (2013) Anal Chem 85:3561–3569
13. Zhou X, Nie H, Yao Z, Dong Y, Yang Z, Huang S (2012) Sens Actuators B Chem 168:1–7
14. Zhang X, Wang L, Ji R, Yu L, Wang G (2012) Electrochem Commun 24:53–56
15. Zhang Y, Wang Y, Jia J, Wang J (2012) Sens Actuators B Chem 171–172:580–587
16. Ding Y, Wang Y, Su L, Bellagamba M, Zhang H, Lei Y (2010) Biosens Bioelectron 26:542–548
17. Wang JP, Thomas DF, Chen AC (2008) Anal Chem 80:997–1004
18. Yeo I-H, Johnson DC (2001) J Electroanal Chem 495:110–119
19. Tominaga M, Shimazoe T, Nagashima M, Kusuda H, Kubo A, Kuwahara Y, Taniguchi I (2006) J Electroanal Chem 590:37–46
20. Hou C, Xu Q, Yin L, Hu X (2012) Analyst (Cambridge, U K) 137: 5803–5808
21. Dong XC, Xu H, Wang XW, Huang YX, Chan-Park MB, Zhang H, Wang LH, Huang W, Chen P (2012) ACS Nano 6:3206–3213
22. Lee KK, Loh PY, Sow CH, Chin WS (2012) Electrochem Commun 20:128–132
23. Novoselov KS, Geim AK, Morozov SV, Jiang D, Zhang Y, Dubonos SV, Grigorieva IV, Firsov AA (2004) Science 306:666–669
24. Feng XM, Li RM, Ma YW, Chen RF, Shi NE, Fan QL, Huang W (2011) Adv Funct Mater 21:2989–2996
25. Cao L, Liu Y, Zhang B, Lu L (2010) Appl Mater Interfaces 2:2339–2346
26. Wu G, Wu Y, Liu X, Rong M, Chen X, Chen X (2012) Anal Chim Acta 745:33–37
27. Hu Y, Jin J, Wu P, Zhang H, Cai C (2010) Electrochim Acta 56:491–500
28. Li SJ, Shi YF, Liu L, Song LX, Pang H, Du JM (2012) Electrochim Acta 85:628–635
29. Zhao Y, Song X, Song Q, Yin Z (2012) CrystEngComm 14:6710–6719
30. Yuan B, Xu C, Deng D, Xing Y, Liu L, Pang H, Zhang D (2013) Electrochim Acta 88:708–712
31. Zhu C, Zhai J, Wen D, Dong S (2012) J Mater Chem 22: 6300–6306
32. Dong X, Ma Y, Zhu G, Huang Y, Wang J, Chan-Park MB, Wang L, Huang W, Chen P (2012) J Mater Chem 22:17044–17048
33. Guo C, Yang H, Sheng Z, Lu Z, Song Q, Li C (2010) Angew Chem, Int Ed 49:3014–3017
34. Xie J, Cao H, Jiang H, Chen Y, Shi W, Zheng H, Huang Y (2013) Anal Chim Acta 796:92–100
35. Xiang C, Li M, Zhi M, Manivannan A, Wu N (2013) J Power Sources 226:65–70
36. Wang J, Zhou J, Hu Y, Regier T (2013) Energy Environ Sci 6:926–934
37. Kovtyukhova NI, Ollivier PJ, Martin BR, Mallouk TE, Chizhik SA, Buzaneva EV, Gorchinskiy AD (1999) Chem Mater 11:771–778
38. Salimi A, Hallaj R, Soltanian S, Mamkhezri H (2007) Anal Chim Acta 594:24–31
39. Salimi A, Mamkhezri H, Hallaj R, Soltanian S (2008) Sens Actuators B Chem 129:246–254
40. Xia C, Ning W (2010) Electrochem Commun 12:1581–1584
41. Wang G, Wei T, Zhang W, Zhang X, Fang B, Wang L (2010) Microchim Acta 168:87–92
42. Wang CX, Yin LW, Zhang L, Gao R (2010) J Phys Chem C 114: 4408–4413
43. Wang X, Hu C, Liu H, Du G, He X, Xi Y (2010) Sens Actuators B Chem 144:220–225
44. Kung CW, Lin CY, Lai YH, Vittal R, Ho KC (2011) Biosens Bioelectron 27:125–131